Application of an index of sediment connectivity in a lowland area

Aurore Gay, Olivier Cerdan, Vincent Mardhel & Marc Desmet

Journal of Soils and Sediments

ISSN 1439-0108

J Soils Sediments
DOI 10.1007/s11368-015-1235-y

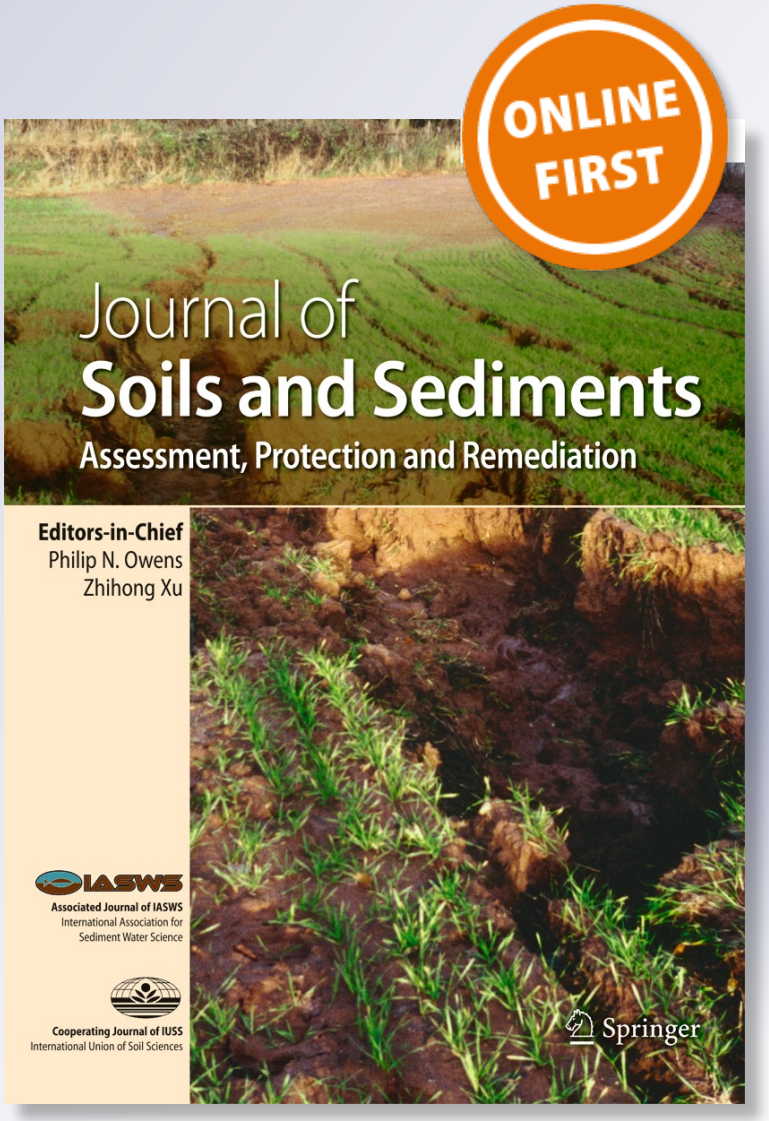

Springer

J Soils Sediments
DOI 10.1007/s11368-015-1235-y

SEDIMENTS, SEC 3 • HILLSLOPE AND RIVER BASIN SEDIMENT DYNAMICS • RESEARCH ARTICLE

Application of an index of sediment connectivity in a lowland area

Aurore Gay[1,2] · **Olivier Cerdan**[1] · **Vincent Mardhel**[1] · **Marc Desmet**[2]

Received: 14 February 2015 / Accepted: 5 August 2015

Abstract
Purpose Sediment connectivity at the landscape scale has gained interest in the last few decades. Distributed approaches, such as topographic indices, are widely used to evaluate this connectivity. However, most of the research efforts are concentrated in mountainous areas while little work has been done in lowland areas where evidence of high connectivity has been reported. The objectives of this study are as follows: (i) to integrate landscape infiltration/runoff properties in the assessment of connectivity to account for lowland processes and (ii) to apply this approach to a large territory with both mountainous and lowland areas.
Materials and methods The topographic index of connectivity (*IC*) of Borselli et al. (2008) was computed for the Loire–Brittany River Basin (>10^5 km^2). A distributed parameter (*IDPR*) that reflects landscape infiltration and saturation properties due to underlying geological formation characteristics is introduced. We integrated this parameter in a revised index ($IC_{revised}$) as an indicator of landscape hydrologic connectivity. Results at the pixel scale are aggregated at the watershed scale.
Results and discussion Two maps of connectivity are produced, considering the initial IC and the revised form ($IC_{revised}$). As expected, the *IC* gives the highest connectivity in the steepest areas and does not reflect the existing connectivity in lowland areas. On the contrary, the $IC_{revised}$ computed in this study profoundly modifies the sediment connectivity values. These changes are evenly distributed over the entire territory and affected 51.5 % of the watersheds. As a result, we obtained a better correlation between calculated connectivity and the observed drainage density (which reflects the actual connections between hillslopes and rivers) in areas where slopes are gentle (<7 %).
Conclusions Topographic indices do not reflect the real sediment connectivity in lowland areas, but their adaptation by considering runoff processes of such areas is possible. The $IC_{revised}$ presents an interesting perspective to define other highly connected areas at the country scale, as 17 % of the French territory is characterized by very gentle slopes with high runoff capacity.

Keywords Connectivity · *IDPR* · Loire river · Lowland areas

1 Introduction

Sediment and flow connectivity, i.e., "the internal linkages between runoff and sediment generation in upper parts of catchments and the receiving waters" (Croke et al. 2005), are a key attribute in the study of sediment redistribution within the landscape. Because on-site and off-site effects of such redistribution are detrimental to environmental systems and populations, the comprehension and assessment of the spatial variability of soil erosion and sediment delivery processes are a long-standing effort and are still today a central topic of researches (Haregeweyn et al. 2013; Bisantino et al. 2015). The recent emergence of the connectivity framework and associated tools has provided a new framework for the study of landscapes and soil redistribution processes (Bracken

Responsible editor: Rajith Mukundan

✉ Aurore Gay
aurore.gay73@gmail.com

[1] BRGM, 3 avenue Claude Guillemin, 45060 Orléans Cedex 2, France

[2] GéHCO, Université François Rabelais, Parc de Grandmont, 37200 Tours, France

Published online: 21 August 2015

et al. 2013, 2015) and for the implementation of effective sediment trapping measures (Mekonnen et al. 2014). As a consequence, considerable progress in quantifying connectivity at various spatial scales has been achieved, and different methodologies have been developed. For example, at the plot to hillslope scale, functions (Western et al. 2001) and indicators (Darboux et al. 2001; Antoine et al. 2009) have been developed to assess connectivity. At the hillslope to the catchment scale, the sediment connectivity can be inferred using conceptual frameworks: for example, the sediment delivery ratio (*SDR*, Walling 1983) is the ratio between gross and net erosion and has been used to provide a first evaluation of the catchment connectivity (Brierley et al. 2006; Baartman et al. 2013). Sediment budgets (Bracken and Croke 2007; Walling and Collins 2008) and indicators, e.g., the drainage density (Delmas et al. 2009) and the wetness index (Ali et al. 2013), can also be used to provide finer insight into the catchment connectivity. However, to evaluate the sediment contribution from the different areas of the catchment, more distributed approaches are needed, e.g., the graph theory (Heckmann and Schwanghart 2013) and topographic indices (e.g., Lane et al. 2009). The latter have been widely used (e.g., Reid et al. 2007; Lane et al. 2009) as they require very few data, allowing for the evaluation of connectivity where field campaigns are not easy to carry out, such as in remote areas or for large territories.

Recently, Borselli et al. (2008) have developed a GIS-based index relying on topography derived from a Digital Terrain Model (DTM) and on land use. The index provides information on the potential connections between source areas and local sinks. Generally, this index has met with great success in the scientific community for its easy handling, the very few data needed for implementation, and its complementarity with field observations. The index has been successfully applied to medium-size catchments ($\leq 10^2$ km^2) in Italy by the same authors and has been used by other authors for similar-size catchments and for different purposes, such as the following: to assess the influence of land use change on connectivity in Spain (López-Vicente et al. 2013; Foerster et al. 2014), to track contaminated sediment dispersion in Japan (Chartin et al. 2013), and to identify hot spots of primary sediment sources to permanent sinks in an Australian semi-arid area (Vigiak et al. 2012) and in the Mediterranean basin (e.g., Sougnez et al. 2011).

Nevertheless, Borselli et al. (2008) stressed that soil surface characteristics that influence runoff processes within a watershed or a hillslope should be also considered. For this purpose, adjustments have been proposed by Cavalli et al. (2013) in order to account for the following: (i) soil surface characteristics, by introducing a roughness index as a weighing factor, and (ii) for mountainous transfer properties such as debris flows and channelized sediment transfers. Such modifications allow for the consideration of different types of sediment transport processes that may be hydrologically controlled or not (Bracken et al. 2015). This new version of the index has been applied in Italy (by the same authors), in Turkey (D'haen et al. 2013), and in Switzerland (Meßenzehl et al. 2014).

By definition, topographic indices are based on the concept that the routing of the sediment is driven by the slope steepness and direction. In Borselli's index of connectivity (*IC*), the probability that sediment arriving at point A will reach point B via overland flow processes is based on upstream and downstream characteristics of point A. The index combines both perspectives in a fraction in which the slope parameter plays a role in each of the upstream and downstream characteristics. In contrasting catchments, the application of such an index will reveal high connectivity in the hilly areas, whereas in the valleys, the connectivity will be low. However, in flat areas (e.g., large floodplains, lowland catchments), the use of an index exclusively based on topography may not reveal hot spots of connectivity because factors other than topography control the (dis)connectivity between the different points (Fryirs et al. 2007; Ali et al. 2013).

Yet, most of the studies dealing with connectivity have been achieved in catchments where sediment is transported rapidly during a rainfall event, where the runoff is Hortonian-type (Horton 1945) and where human intervention on the landscape is negligible (e.g., mountainous areas, semi-arid areas). This concentration of research efforts on connectivity in these particular areas has already been highlighted by Bracken et al. (2013), and the main reason for this interest in these catchments is their high sediment yield. In contrast, in lowland areas where sediment yields are often lower (Gay et al. 2014), and where intensive agriculture is predominant and runoff can be generated by soil saturation, little work has been done to incorporate these characteristics in the sediment connectivity assessment. Still, the clogging of numerous French lowland rivers and lakes (e.g., Landemaine et al. 2015; Foucher et al. 2015) points out that connectivity between sediment sources and rivers is a key component in soil redistribution.

In this context, the objective of the present paper is to provide an evaluation of sediment connectivity for a lowland territory. The assessment of the hillslope sediment connectivity is achieved through the use of a sediment connectivity index, based on the one proposed by Borselli et al. (2008), with process and scale constraints: (i) landscape infiltration and saturation properties of lowland areas are integrated in the index and (ii) the assessment is performed over a large river basin (~10^5 km^2) containing both mountainous and lowland areas.

2 Materials and methods

2.1 Study area

The French metropolitan territory is divided into six river basin districts, and for each district, a river basin agency is in charge of the water resources. The Loire–Brittany River Basin (*LBRB* hereafter) is one of the districts and represents 28 % of the territory (~155,000 km^2). From a hydrological and administrative viewpoint, the basin is divided into 2122 small watersheds. Their areas vary from 0.3 km^2 for a lake and its close surroundings to 1492.9 km^2 for the Conie River and its tributaries (Beauce region). This division is generally used for decision making. Therefore, the results are presented at this spatial scale (Degan et al. 2015).

Figure 1 displays the slopes and land use characteristics and geological regions of the study area. From a geological viewpoint, the center of the *LBRB* lies on the sedimentary formations of the Parisian basin and the Aquitaine basin. This area is primarily dominated by croplands, dedicated to intensive farming, on gentle slopes (maximum=66.2 %, mean=3.1 %). The eastern and western parts of the study area lie on old granitic formations. To the east, the Massif Central includes a mountainous area with steep slopes (maximum=134.7 %, mean=10.5 %) dominated by pastures and forests, the highest point of the study site (1849 m), and a gentler area with croplands, the Limagne basin. In contrast, the Armorican basin in the western part of the *LBRB* is a rolling landscape (maximum altitude=385 m) and displays gentler slopes (maximum=86.9 %, mean=4.5 %) and is dominated by croplands and pastures.

2.2 Index of hillslope sediment connectivity

2.2.1 Database and pretreatments

In order to compute the index of connectivity of Borselli et al. (2008), we used three types of data:

(a). The surface water network is provided by the BDCarthage 2013® (available at http://services.sandre.eaufrance.fr/telechargement/geo/BDCarthage/FXX/). This database is a GIS vector layer which provides information on all surface waters within the French territory. It covers both the entire river network and lakes/ponds, and these data were transformed into raster (cells of 50*50 m).

(b). The topographic data, i.e., the slope, the contributing area, and the length to the river network, were calculated using the digital elevation model (DEM) at a 50-m resolution from the BD Alti® IGN. This DEM was derived from the digitization of contour lines taken from maps at 1:25,000 and 1:50,000 and aerial photographs at 1:20,000, 1:30,000, and 1:60,000. In order to ensure the continuity of flow through the landscape, the depressions were filled using the Spatial Analyst algorithm. Moreover, as in some flat areas, the real and theoretical drainage networks do not strictly coincide, we forced the flow direction of the DEM using the raster of the real drainage network and then calculated the values of the contributing area and the length to the river network from this forced DEM.

(c). The land use type was determined using the map from Degan et al. (2015) who combined information from the Référentiel Parcellaire Graphique 2010 (RPG2010 available at https://www.data.gouv.fr/fr/datasets/registre-parcellairegraphique-2010-contours-des-ilots-culturaux-et-leur-groupe-de-culturesmajorita/) and Corine Land Cover 2006. The RPG2010 is a GIS vector layer computed from farmer declarations on the location of their farms and the type of crops. The precision is of 1:5000. The layer was rasterized (cells of 50*50 m) and superimposed with the Corine Land Cover raster in order to complete missing data (e.g., urban areas and forests).

2.2.2 Computation of the index of connectivity

Our approach of hillslope connectivity mapping is based on the *IC* developed by Borselli et al. (2008). The *IC* is pixel-based and represents the probability that sediment within an area will reach a defined target (sinks). The target is defined by the users and can either be the outlet of a catchment or a water system. In this paper, we only consider the sediment connectivity from hillslopes to river channels/lakes. A mask is thus applied on rivers and lakes. The index was computed on ArcGIS10 using the Spatial Analyst extension. The index takes the form:

$$IC = log10\left(\frac{D_{up}}{D_{dn}}\right) \quad (1)$$

with D_{up} the upslope component and D_{dn} the downslope component. The *IC* is a dimensionless measure within the [−∞; +∞] range.

The upslope component represents the potential for downward routing of the sediment produced in the upslope contributing area of each cell and was calculated as follows:

$$D_{up} = \overline{W}\cdot\overline{S}\cdot\sqrt{A} \quad (2)$$

where $\overline{W}$ is the average weighing factor of the upslope contributing area (dimensionless), $\overline{S}$ is the average slope gradient of the upslope contributing area (m/m), and A is the upslope contributing area (m^2). The downslope component D_{dn}

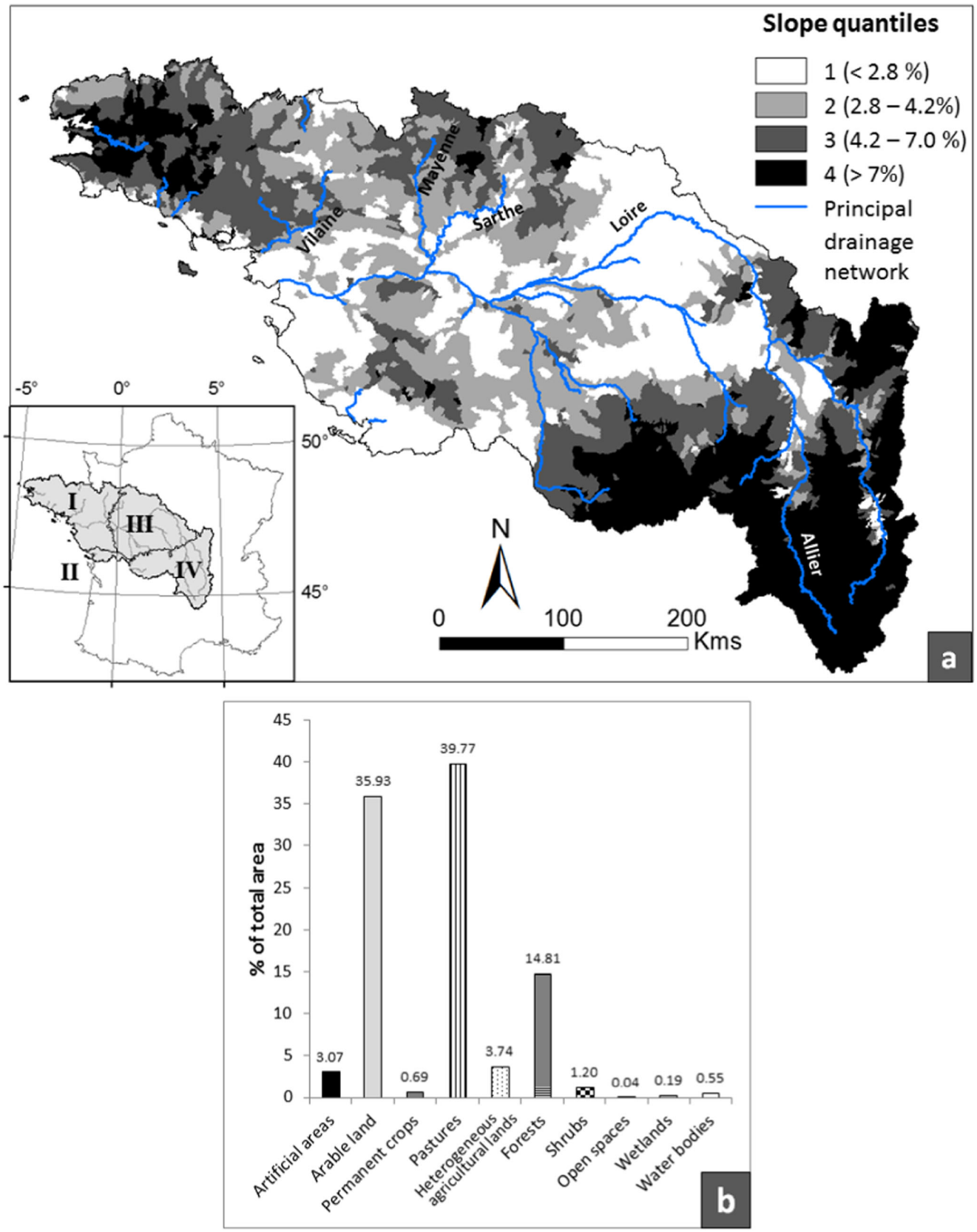

Fig. 1 Characteristics of the Loire–Brittany River Basin, France. **a** Mean slope values per watershed and location of the study area. Roman numerals indicate the four geological regions: I, Armorican basin; II, Aquitaine basin; III, Parisian basin; and IV, Massif Central. **b** Land use statistics from the combination of the CLC2006 and the RPG 2010 (Degan et al. 2015, see text for details)

represents the weighted flow path length of the transported sediment to the nearest sink targeted by the users (water systems in our case) and is calculated as follows:

$$D_{dn} = \sum_i \frac{d_i}{W_i \cdot S_i} \quad (3)$$

where d_i is the length of the i^{th} cell along the downslope path (in m), W_i is the weight of the i^{th} cell (dimensionless), and S_i is the slope gradient of the i^{th} cell.

The weighing factor W is introduced in the index by Borselli et al. (2008) to account for the local conditions of the landscape. The authors set its value according to the *C-factor* of USLE/RUSLE models (Wischmeier and Smith 1978; Renard et al. 1997) that is the crop/vegetation and management factor used to determine the relative effectiveness of crop management systems in terms of soil loss. We used the same values as the ones proposed by those authors for the different land use types.

2.3 Adaptation of the index of connectivity for lowland area

At the watershed scale, the hydrologic connectivity can be inferred from the drainage density (Delmas et al. 2009). This parameter is calculated as the ratio between the length of the hydrographic network to the watershed area and is expressed in km.km^{-2}. In this study, we introduce a pixel-based parameter (*IDPR*) related to the drainage density and which accounts for hydrological connectivity. This parameter characterizes the landscape in terms of soil infiltration/runoff. In this section, we describe the computation of the *IDPR*, the rescaling of the values, and the integration of the parameter in the original *IC* as a weighing factor.

2.3.1 Hillslope hydrologic connectivity parameter

The index of development and persistence of the drainage network (*IDPR*, Indice de Développement et Persistance des Réseaux) was developed by Mardhel et al. (2004) and has been recently modified. This index supports the assumption that the organization of the drainage network is dependent on the underlying geological formations. In a homogeneous environment, only the slope and relief forms guide the development of the hydrographic network while in natural landscapes, the geological formations play an important role in the development of this hydrographic network. Indeed, lands overlying permeable material display a sparse hydrographic network (and thus a low drainage density) as water infiltrates, while in lands overlying impermeable rocks, the hydrographic network is important, and the drainage density is high.

The *IDPR* allows the comparison of the theoretical river network established due to morphological parameters only (homogeneous environment) and the real river network that has developed under heterogeneous geological conditions. This distributed index characterizes each landscape unit (raster cell in this study) in terms of its distance to the theoretical river network and to the real river network along the flow path. The distance to the theoretical river network is calculated using the raw DEM, and the network of thalwegs is extracted automatically thanks to an algorithm (Mardhel and Gravier 2006). The distance to the real river network is calculated using the river network from the BDCarthage and the DEM. In order to ensure the continuity of the flow through the landscape, the depressions of the DEM are filled. The *IDPR* is calculated according to the following:

$$IDPR = \frac{\begin{array}{c}\textit{The least cumulative cost distance for each cell to}\\ \textit{the nearest theoretical water course over the slope surface}\end{array}}{\begin{array}{c}\textit{The least cumulative cost distance for each cell to}\\ \textit{the nearest real water course over the slope surface}\end{array}} \quad (4)$$

The *IDPR* values range from 0 to +∞. Values <1000 suggest that waters running off the slopes reach a theoretical network before they reach the real hydrographic network. This result thus indicates that the underlying rock formations are permeable and that infiltration is the dominant process. On the contrary, values >1000 indicate a denser real river network than the theoretical one. This implies that runoff is the dominant process. A value of 1000 represents a strict balance between infiltration and runoff as there exists a compliance between the availability of the real and theoretical hydrographic networks. In order to simplify this index, the values are arbitrarily limited to 2000. Lands with *IDPR* values >2000 are assimilated to wetlands.

In mountainous areas, the drainage density and the *IDPR* values are very high. In these regions, runoff is important and is mostly governed by the steep slopes. Therefore, the *IDPR* parameter is redundant with the slope information already contained in the IC. Thus, we chose not to take this parameter into account in these areas. For pixels with a steeper slope than 7 % (Delmas 2011), the *IDPR* was not taken into account into the calculation of *IC*.

The use of the *IDPR* as an indicator of hydrologic connectivity presents several advantages. First, it is a distributed parameter that can be integrated directly into the *IC* as its resolution corresponds to the same cell size as the two other input data (DEM and land use map). Second, it allows for the substitution of numerous data on geological and soil/subsoil properties while taking these parameters into account in the evaluation of connectivity. Third, it is not only topography-based and can reflect flat areas prone to rapid soil saturation. Finally, the *IDPR* has proven to be a good indicator of hydrologic connectivity at the catchment scale in the *LBRB* and in France (Dupas et al. 2015).

2.3.2 Reclassification values of the IDPR

In the same way as the *W* factor displays values between 0 and 1, the hydrologic connectivity factor, the *IDPR*, should display the same range of values. Therefore, the initial *IDPR* values are rescaled to the range [0, 1] with values of 1 representing full connectivity due to high runoff, and 0 as low connectivity due to high infiltration properties. In order to avoid zeros and infinite values in Eq. (6), we set a threshold of 0.1 to null *IDPR* values. The frequency of occurrence of the *IDPR* values takes a trimodal distribution form with peaks at the extreme values of 0 and 2000 and a third peak centered on the 1000 value. Two types of rescaling are investigated.

First, we rescaled the *IDPR* values according to the 1:1 line into $IDPR_{linear}$ (Eq. (5), Fig. 2). Second, in order to stretch the extreme values of the *IDPR* and thus highlight areas characterized by high infiltration or saturation properties, we rescaled the values according to a sigmoid curve into $IDPR_{sigmoid}$ (Eq. (5), Fig. 2).

$$\begin{cases} IDPR_{linear} = \dfrac{IDPR}{2000} \\ IDPR_{sigmoid} = \dfrac{1}{1 + e^{-a(IDPR-c)}} \end{cases} \quad (5)$$

where a is a lumped parameter, which we arbitrarily set to 0.035. Assuming that the 1000 value of the *IDPR* (corresponding to infiltration/runoff of same importance) represents the mean connectivity, we assigned a hydrologic connectivity value of 0.5 in both cases.

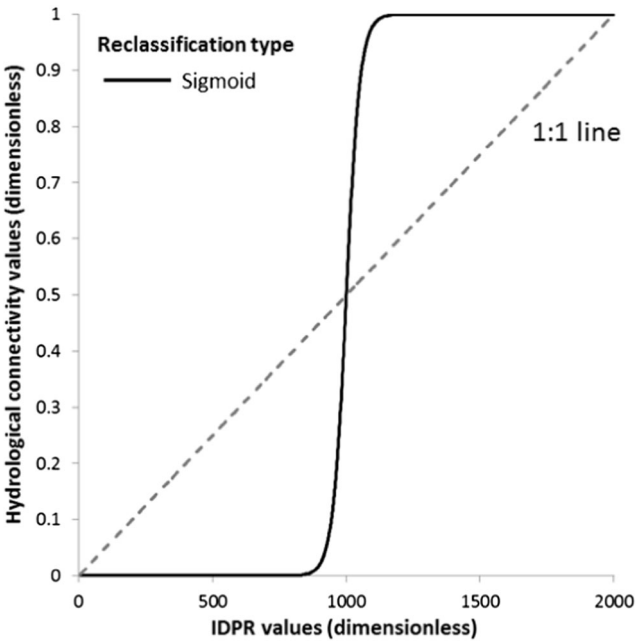

Fig. 2 Hydrologic connectivity values from the reclassification of the index of development and persistence of the drainage network (*IDPR*) according to a sigmoid function and to the 1:1 line

Finally, we included the resampled values of the *IDPR* in a $IC_{revised}$ as follows:

$$IC_{revised} = log10\left(\frac{\overline{W}\cdot\overline{IDPR}\cdot\overline{S}\cdot\sqrt{A}}{\sum_i\left(\frac{d_i}{W_i\cdot S_i\cdot IDPR_i}\right)}\right) \quad (6)$$

where $\overline{IDPR}$ is the average weighing factor of the upslope contributing area and $IDPR_i$ is the weight of the i^{th} cell.

3 Results and discussion

Generally, the *IC* and $IC_{revised}$ are dimensional estimations of the basin connectivity. The values obtained via the computation of both indices are provided for information purposes only. Both indices were applied to the entire *LBRB*, considering the permanent channel network and lakes as targets for sediment. The results are presented both at the pixel scale and at the watershed scale.

3.1 Modeling results from Borselli's index

The pixel values of connectivity range from −12.61 to 1.31 (mean=−6.04, SD=1.92), and the mean connectivity values per watershed range from 10.02 to −3.87. Figure 3a displays the map of mean connectivity values for each watershed, for which the values are ranked in four classes according to quartile boundaries, and a zoom on a certain region at the pixel scale is proposed. At both scales, important regional differences exist. Indeed, the highest mean connectivity values are observed in the eastern and western parts of the territory and the lowest values in the center. The limits between these three areas correspond to those of the geological formations (Fig. 1a) and of the slopes. Figure 3b presents the relationship between the mean connectivity values and the mean slope values. A weak but significant correlation ($p<0.0001$) is found between both variables. This relation takes a logarithmic form. As expected, the steeper the slopes are, the higher the connectivity is. In contrast, no correlation is found between the mean connectivity values of the watersheds and their drainage density (Fig. 3c).

As expected at the pixel scale, for the entire *LBRB*, the highest values of connectivity are found close to the river network while the lowest values are found in more distant regions. Finer variations in connectivity patterns can also be observed. Indeed, the area north of the Loire River (corresponding to the Beauce region) appears more connected than the area south of the river (corresponding to the Sologne

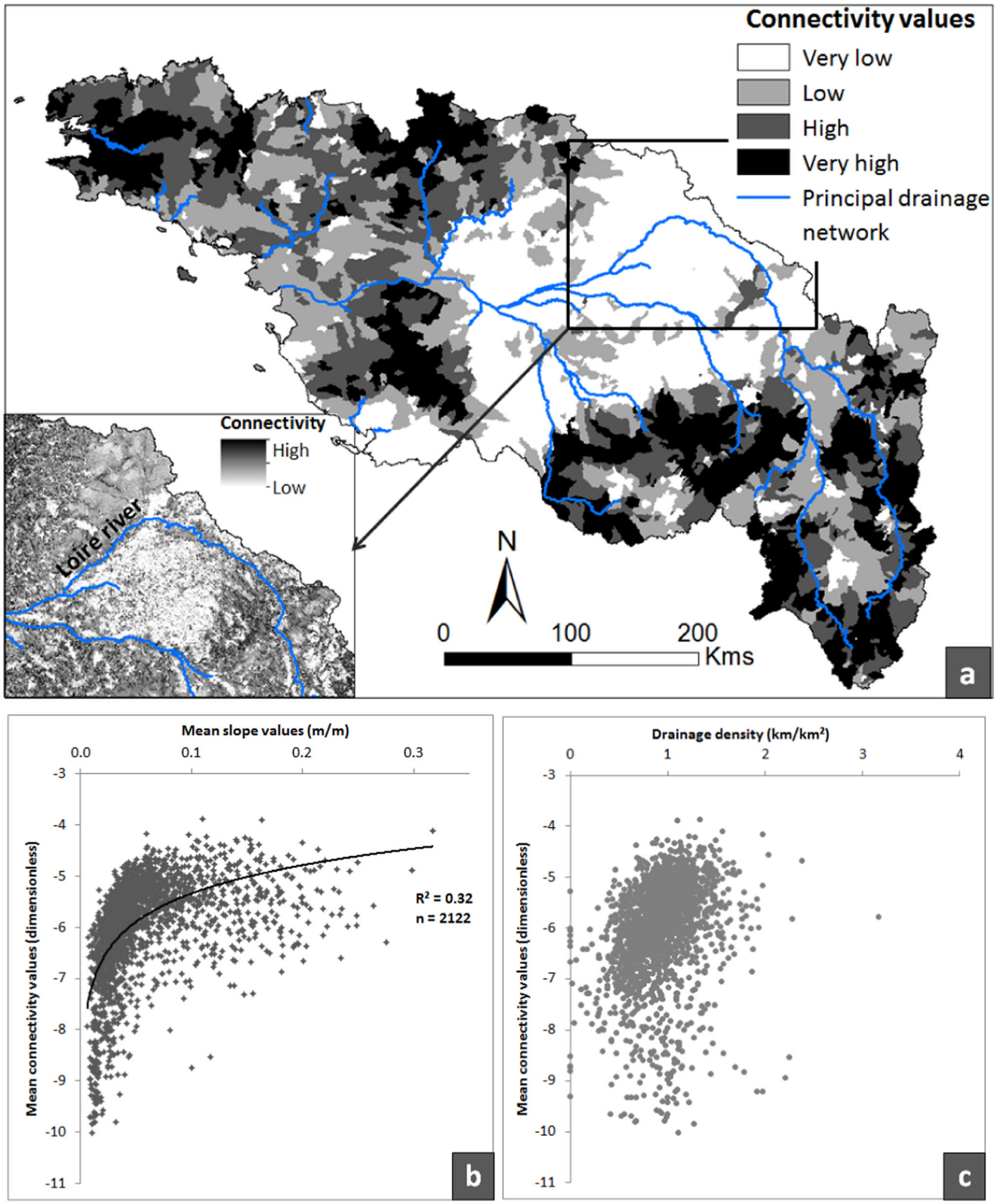

Fig. 3 Sediment connectivity from hillslope to water system according to the index of connectivity (*IC*) (Borselli et al. 2008). **a** Map of the mean connectivity for each watershed, the values are ranked according to quartile classes, and zoom at the pixel size on the Beauce and Sologne regions (see text); **b** Relationship between the mean connectivity and the mean slope per watershed; and **c** Relationship between the mean connectivity and the drainage density per watershed

region). These two regions display similar mean slope values (<2 %), and the driving factor for connectivity differences between both areas is the land use type (*W* factor), as the Beauce region is primarily agricultural while the Sologne region is dominated by forests.

From these results, two conclusions may be drawn. First, to our knowledge, this is the first time that the *IC* is computed for such a large territory. Indeed, in other studies, the order of magnitude of catchment size does not exceed 10^3 km^2, and the DEM resolution is fine (from 2.5- to 20-m grid). In our case, the computation is done with a lower resolution DEM (50-m grid) over more than 10^5 km^2. Despite those two constraints, the *IC* is applicable and allows for the discrimination of areas that are supposed to be more connected than others.

Second, as expected, steeper areas appear more connected than those of lowland areas. However, some regions, such as the Sologne, are primarily composed of wetlands with an important network of ditches. In these places, hillslopes are therefore highly connected to the main channel system. However, their connectivity values from the *IC* are among the lowest ones of the *LBRB*. Similarly, pond and river clogging are evidence of the high connectivity in upstream areas and deposition in downstream parts. Several problems of such clogging have been reported by the River Basin Agency (Bourrain, personal communication 2014) in areas where the connectivity is given by the *IC* as low. Of course, these results do not call into question the efficiency of the *IC*, which can be used directly as a first approach for connectivity assessment, but clearly highlights the lack of consideration of lowland processes in sediment transfers.

3.2 Connectivity from the revised index and comparison with initial index

A distributed parameter, the *IDPR*, accounting for landscape infiltration and saturation properties is introduced as one of the weighing factors in the *IC* (see Sect. 2.3). Two rescaling approaches of this parameter are proposed taking a linear ($IDPR_{linear}$) and a sigmoid ($IDPR_{sigmoid}$) form. We first present the results obtained at the pixel and watershed scale in the $IC_{revised}$ when introducing the $IDPR_{sigmoid}$. We then discuss these results and differences obtained with $IC_{revised}$ when introducing the $IDPR_{linear}$.

3.2.1 Connectivity at the pixel scale

At the pixel scale, the connectivity values from the $IC_{revised}$ range from −42.89 to 1.31, with a mean value of −13.58 (SD= 10.07) representing a decrease by −7.54 of the mean value. As expected, for most cells, the connectivity has decreased due to the introduction of the *IDPR* values in the range of [0, 1]. For a few cells (0.21 %), the connectivity has increased.

Figure 4 presents the frequency of connectivity values using a step of 0.5. While the *IC* curve displays a single and high peak around the −6.0 value, the $IC_{revised}$ curves display two peaks. For the $IC_{revised}$ with $IDPR_{sigmoid}$, the first peak is high and around −6.0, while the second is smoother and around −23.0. Similarly, for the $IC_{revised}$ with $IDPR_{linear}$ values according to the 1:1 line, the first peak is around −6.5, and the second peak is around −10.5. In all three cases, the peak around 6.0 and −6.5 corresponds to cells close to the channel network (within a distance of ~500 m around the river), while in the case of a second peak, it corresponds to areas further away from rivers or to small subcatchments directly (dis)connected to the river system. Therefore, the introduction of the $IDPR_{sigmoid}$ strongly modifies the distribution of the connectivity values. Moreover, when looking at the zoom in Fig. 5, we note that the trend in connectivity has reversed: the cells in the Beauce region with high infiltration properties, due to underlying karstified limestones, are less connected than the ones in the southern region, the Sologne, where the drainage density is high as soils are easily saturated due to an impermeable layer of clay. Therefore, for the same slope values, while the dominant factor for connectivity in the *IC* is the land cover in this area, the $IDPR_{sigmoid}$ takes over this factor in the $IC_{revised}$.

Table 1 presents some connectivity values (minimum, maximum, mean, and standard deviation) mapped with the *IC*, the $IC_{revised}$, and from the difference between both, for different land use types (arable land, pastures, and forests)

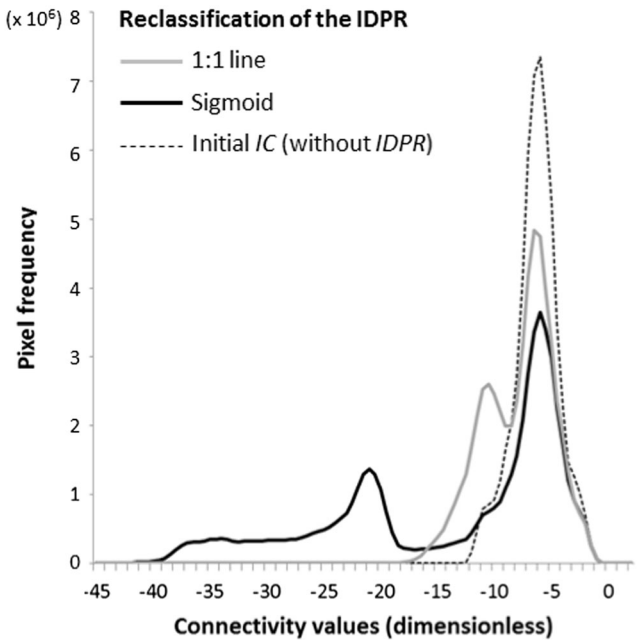

Fig. 4 Comparison of the frequency of connectivity values at the pixel scale from the initial index of connectivity (*IC*) and the $IC_{revised}$ using a sigmoidal rescaling of the index of development and persistence of the drainage network (*IDPR*) values or a linear rescaling (1:1 line)

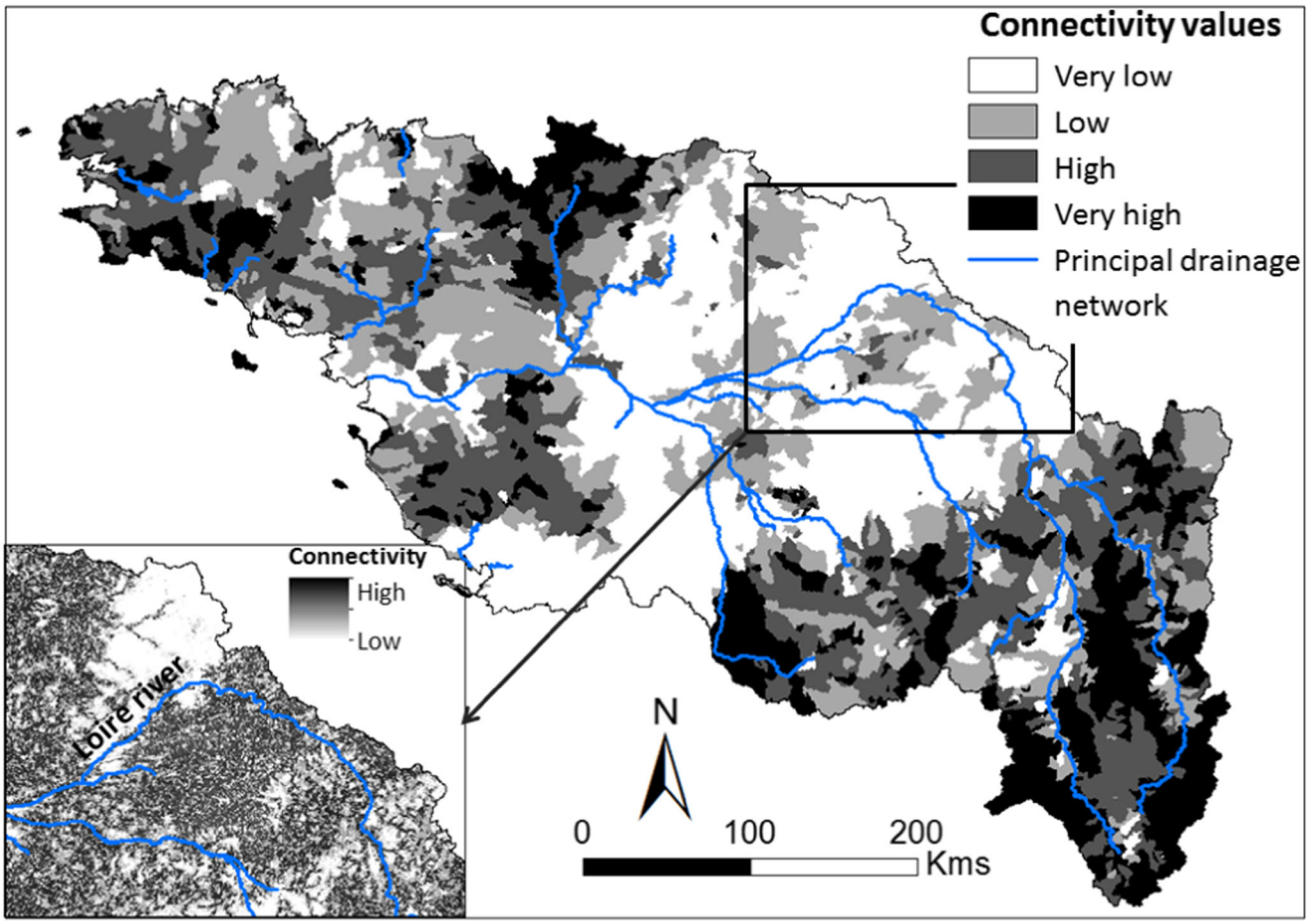

Fig. 5 Map of mean connectivity for each watershed (classification of mean values in quartiles)

Table 1 Connectivity values (minimum, maximum, mean and standard deviation) per land use type and slope classes according to the initial index of connectivity (*IC*) and the $IC_{revised}$ and the differences between both

Slope classes												
	<2 %			2 to 5 %			5 to 7 %			>7 %		
	IC	$IC_{revised}$	Difference	IC	$IC_{revised}$	Difference	IC	$IC_{revised}$	Difference	IC	$IC_{revised}$	Difference
Arable lands (%)	15.66			11.60			3.40			4.06		
Min	−10.85	−41.04	−30.70	−10.28	−39.77	−30.40	−9.575	−39.77	−30.40	−9.32	−25.05	−19.33
Max	−0.88	−1.58	3.55	−0.91	−1.00	4.22	−0.89	−1.01	4.51	−0.02	−0.02	3.66
Mean	−6.77	−19.31	−12.54	−5.84	−15.03	−9.19	−5.23	−12.12	−6.89	−4.75	−8.86	−4.20
SD	1.21	11.55	10.96	1.17	10.25	9.63	1.17	8.97	8.39	1.28	6.88	6.17
Pastures (%)	10.74			12.36			5.36			11.52		
Min	−10.55	−40.48	−31.09	−10.18	−39.54	−30.40	−9.60	−39.19	−30.40	−9.57	−24.90	−17.62
Max	−0.93	−1.20	4.12	0.04	−0.04	4.09	−0.05	−0.56	3.95	0.23	0.18	4.95
Mean	−5.00	−14.05	−8.05	−5.25	−12.03	−6.78	−4.77	−10.50	−5.73	−4.29	−7.65	−3.36
SD	1.32	9.85	9.41	1.26	8.94	8.43	1.27	8.24	7.71	1.40	6.45	5.72
Forests (%)	4.61			3.05			1.20			5.95		
Min	−12.61	−42.89	−30.99	−12.00	−42.22	−30.40	−11.48	−41.20	−30.40	−11.16	−27.68	−19.50
Max	−3.23	−3.36	3.50	−2.94	−3.13	2.66	−2.66	−2.76	2.91	−1.88	−1.90	3.11
Mean	−10.08	−19.38	−9.29	−9.10	−17.52	−8.42	−8.41	−15.32	−6.91	−7.31	−10.18	−2.86
SD	1.26	10.13	9.79	1.30	9.60	9.14	1.33	8.90	8.41	1.43	6.05	5.41

and slope classes. The three land use types together correspond to 90 % of the area of the entire territory. The most representative combination is the arable lands on slopes <2 % which corresponds to 15.66 % of the *LBRB* followed by pastures on slope from 2 to 5 % (12.36 % of the territory).

When looking at *IC* and $IC_{revised}$ values, we note that independently from the land use type, the connectivity increases as the slope increases in both cases. This result highlights the importance of the slope factor in the calculation of the indices. However, if the SD values for the IC remain stable independently from the land use type and the slope steepness (between 1.17 and 1.43), the range of SD values for $IC_{revised}$ is wider (between 6.05 and 11.55). In general, the variations decrease as the slope increases. This is primarily due to the fact that the *IDPR* is not taken into account in cells with slopes >7 %. These results confirm that in flat areas, for similar slopes and land use types, the introduction of the $IDPR_{sigmoid}$ leads to strong differences in connectivity values according to soil properties.

More specifically, great differences between the connectivity from both indices exist as the values obtained with the $IC_{revised}$ may be up to three times smaller than the ones obtained with the initial *IC*. This highest variability between both values is observed for arable lands on very gentle slope (<2 %) with a mean difference of −12.54 (SD=10.96). The lowest variability is observed for forests on steep slopes (>7 %) where connectivity values from $IC_{revised}$ are 0.4 times smaller than the ones obtained with the *IC*. The lowest connectivity values are observed for forests on slopes <2 % with a minimum of −12.61 with the *IC* and −42.89 with the $IC_{revised}$. The highest mean connectivity value (−1.31) per land use type obtained with both indices corresponds to inland marshes (not shown in Table 1).

In general, the introduction of the *IDPR* has induced more variation and differences in connectivity values in flat areas than in steep ones, and especially in agricultural lands (arable lands and pastures) than in forested areas. However, other processes than soil saturation may induce variations in sediment and flow connectivity but are not reflected by the *IDPR* or within the *IC*. First, soil crusting can induce high runoff and can thus increase the connectivity of the soil surface (Le Bissonnais et al. 2005a; Kirkby 2014). Second, land management practices such as the implementation of drainage tile networks in agricultural lands in the 1970s has provided arable land with subsurface pathways for water and sediment. Several studies indicate that the contribution of drain tiles to the sediment budget can be up to 15 % for a German catchment (Kiesel et al. 2009) and 55 % for a British catchment (Russell et al. 2001). However, the contribution of such features to sediment connectivity remains unclear, and their inclusion in models is a difficult task that needs attention (Kiesel et al. 2010). In the low connectivity belt at the center of the *LBRB*, arable lands are the dominant land use type (up to 90 % of the surface area), and the percentage of those lands implemented with drained tiles can reach 85.5 % (statistics from the French Ministry for Agriculture, available online at http://agreste.agriculture.gouv.fr/enquetes/recensements-agricoles/recensement-agricole-2010/resultats-donnees-chiffrees/). This area is also prone to soil crusting (Le Bissonnais et al. 2005b). Therefore, the connectivity in this area might be much more important than exposed by the $IC_{revised}$, and research is needed to take account of the described processes in the assessment of connectivity. Furthermore, land use type (Novara et al. 2011; Gao et al. 2014), land management practices such as crop rotation (Gabriels et al. 2003; Foerster et al. 2014) and tillage (Van Oost et al. 2000), and wildfires (Cerdà and Doerr 2010) may participate in the variation of connectivity throughout the year by influencing soil conservation and moisture conditions. At present, no fine distinction is made between the different land use types within the arable land or forest classes. Further researches should therefore concentrate on integrating these agricultural practices and seasonal variations of land cover to provide a better insight into sediment connectivity during the year.

3.2.2 Connectivity at the watershed scale

Figure 5 presents the map of mean connectivity per watershed obtained with the $IC_{revised}$. As before (Sect. 3.1), values are ranked in four classes according to quartile boundaries, and a zoom on the same region at the pixel scale is provided. Mean connectivity values per watershed range from 34.87 to −4.44 (mean=−12.30, SD=4.32). The decrease in mean connectivity values per watershed has changed the boundaries of the quartile classes. From the new map of mean connectivity, we notice that the four classes are homogeneously distributed over the entire territory. Still, the three areas previously described (eastern, center, and western parts) remain identifiable with clear lithological limits and may be explained by the strong relationship between the *IDPR* values and the underlying lithology.

From Fig. 6a, it is clear that a correlation exists (R^2=0.52) between the mean connectivity values from the $IC_{revised}$ and the drainage density. This result was expected as the drainage density strongly depends on the lithology and reflects soil infiltration (Vogt et al. 2007) and connectivity (Delmas et al. 2009). Moreover, there are strong correlations (R^2=0.69, not shown on the graph) between mean *IDPR* values and the mean connectivity values and between the mean *IDPR* values and the drainage density (R^2=0.53, Fig. 6b). This result confirms the interesting potential of the *IDPR* to reflect connectivity in lowland areas.

Figure 7 presents the map of the class differences between the initial *IC* and the $IC_{revised}$ for each watershed. The mean connectivity class remains unchanged for 48.5 % of the

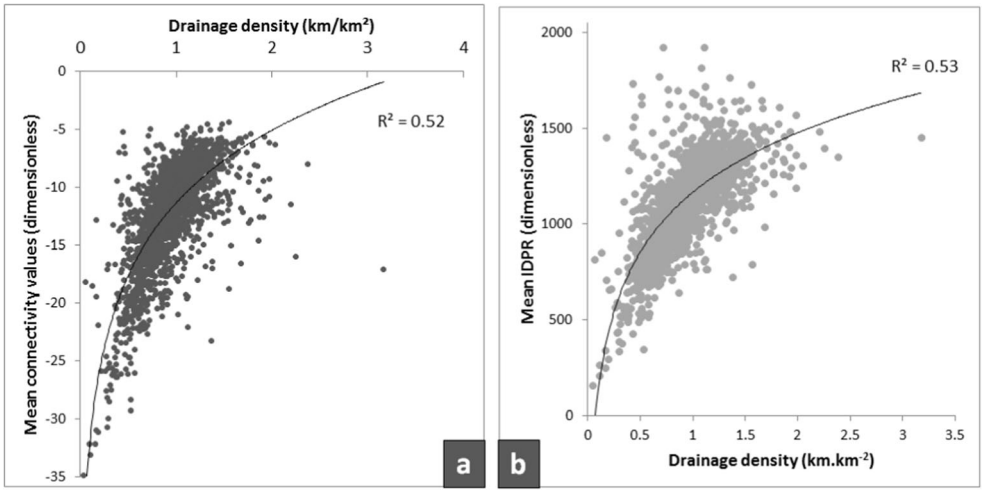

Fig. 6 Relationships per watershed between the drainage density and **a** the mean connectivity values, and **b** the mean index of development and persistence of the drainage network (*IDPR*) values

watersheds. For 61.3 % of them, the connectivity values were already in the highest or the lowest class with the *IC*. In these areas, the *IDPR* confirmed the low connectivity of the landscape, e.g., in karstified limestones of the Beauce region, or the high connectivity of the landscape, e.g., on the volcanic formations at the east of the upstream part of the Allier River.

In contrast, the introduction of the *IDPR* in the $IC_{revised}$ changed the mean connectivity classes for 51.5 % of the watersheds. Even though the positive (increase in connectivity for 24.1 % of the watersheds) and negative (decrease in connectivity for 27.4 % of the watersheds) changes in class difference are evenly distributed in the Loire–Brittany River

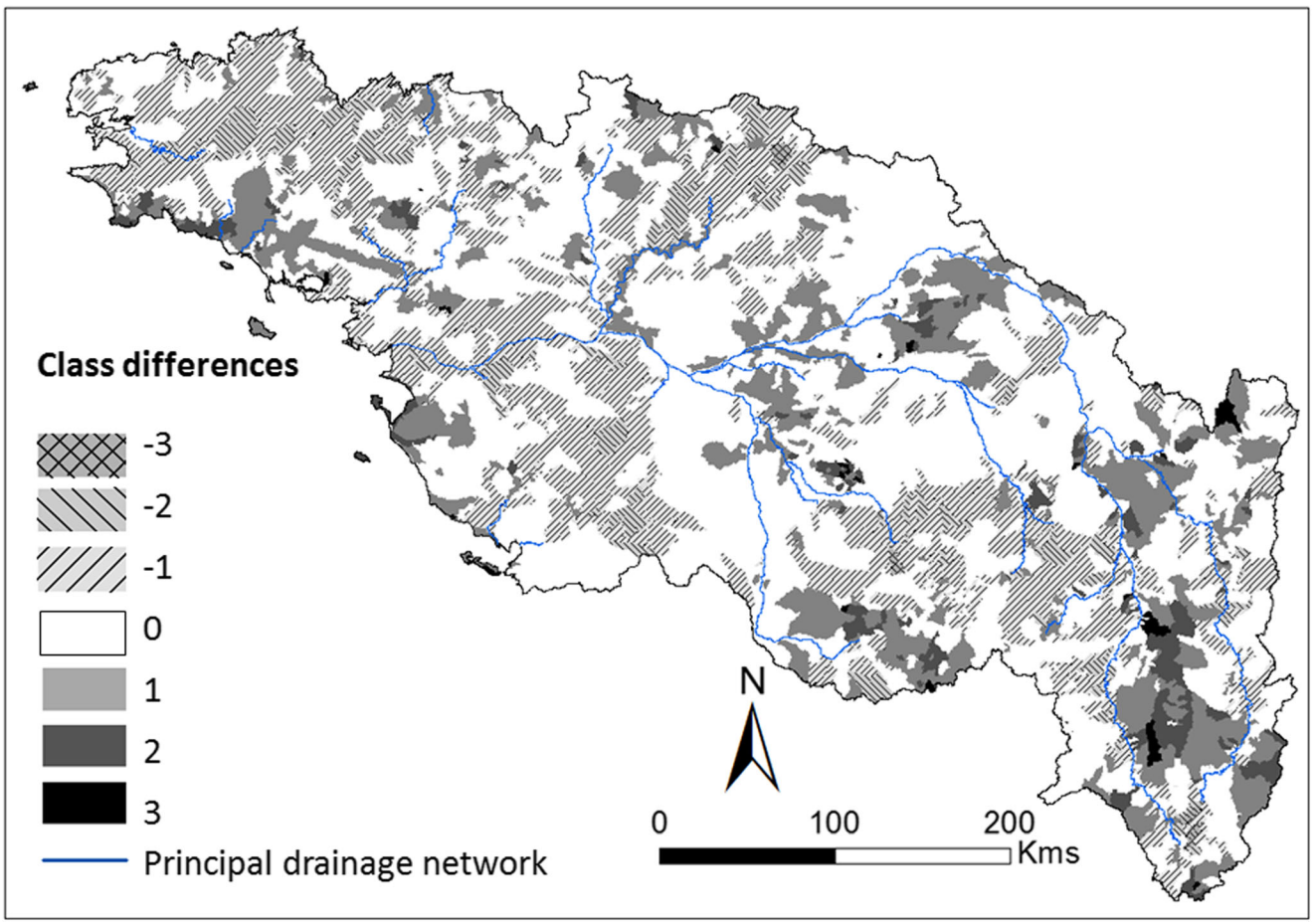

Fig. 7 Map of the class differences between the initial index of connectivity (*IC*) and the $IC_{revised}$ with index of development and persistence of the drainage network ($IDPR_{sigmoid}$)

Basin, some patterns can be distinguished which are closely related to the underlying geological formation characteristics. Indeed, in Vendée, at the south of the Loire outlet, the *IDPR* is very high and expresses the existence of a shallow aquifers and the low infiltration capacity of soils. Moreover, in the Sologne region, and in the Limagne basin at the center of the Massif Central, the high *IDPR* values are related to the presence of impermeable geological formations, respectively, clays of the Cenomanian period and sedimentary formations on a granitic basement with low permeability. In these areas, the connectivity has been increased by two to three classes. On the other hand, the decrease of connectivity corresponds to low values of the *IDPR* which are related to high infiltration due to a high permeability in the fractured bedrock in the north of the Armorican basin or to intense karstification of the sedimentary formations, e.g., in the upstream part of the Loir River basin, at the south east of the Parisan basin. There is, therefore, a great benefit to incorporate factors like the *IDPR* that can account for the nature of the lithology, as all of these changes of connectivity are induced by the landscape's ability to infiltrate (or not) potential overland flow, and as such, they cannot be detected by an index solely dependent on topography.

The relationship between the mean connectivity values from the initial *IC* and $IC_{revised}$ is presented in Fig. 8. The correlation between the mean values from the initial *IC* and $IC_{revised}$ is weak (R^2=0.33). The dispersion of the dots takes a conic form with mean connectivity values relatively similar between both variables when the connectivity is high and a widening of the scatter when the connectivity decreases. Indeed, the mean value from $IC_{revised}$ with $IDPR_{sigmoid}$ can be five times less than the mean value obtained from *IC*. In contrast, when the $IDPR_{linear}$ values are considered in the calculation of the connectivity, a correlation exists between mean connectivity values from the *IC* and the ones from the $IC_{revised}$ (R^2=0.79). The fact that such a correlation exists clearly indicates that the introduction of the $IDPR_{linear}$ values or raw *IDPR* values in the index would just correspond to the addition of an adjustment factor and will not represent the described properties of lowland areas. The rescaling of the *IDPR* values according to a sigmoid curve gives more weight to areas where the infiltration or the saturation is medium to high.

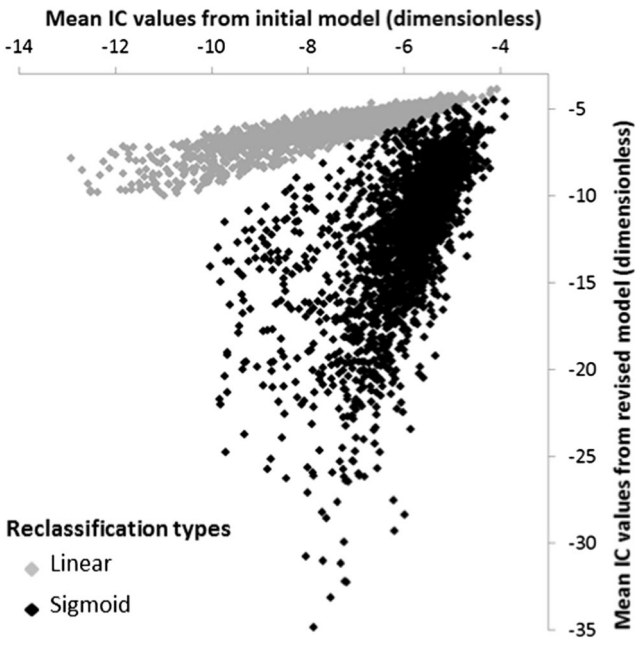

Fig. 8 Relationship between mean connectivity values per watershed from the revised index of connectivity ($IC_{revised}$) with index of development and persistence of the drainage network ($IDPR_{sigmoid}$) and the initial *IC*

Finally, as discussed at the end of Sect. 3.2, the *IDPR* reflects one of the processes characteristic of lowland areas, the soil saturation due to certain underlying lithology. However, in a human-made landscape, such as intensive cultivated areas, anthropic factors play a role in connectivity, and their integration is necessary. Still, the assessment of sediment connectivity over the *LBRB* has helped us to identify hot spots for sediment transfers. The proposed revised index of connectivity at the pixel scale and aggregation of results at the watershed scale shows interesting potential to (i) define priority zones for financial support from stakeholders to implement land and water conservation practices and (ii) determine the appropriate location for sediment trapping measures (Gumiere et al. 2011; Mekonnen et al. 2014).

4 Conclusions, applications, and perspectives

In this paper, we present the application of the sediment index of connectivity (*IC*) of Borselli et al. (2008) to a large territory, the Loire–Brittany River Basin, and its adaptation to take into account lowland runoff processes. A distributed parameter (i.e., *IDPR*) that reflects landscape infiltration and saturation properties is added into a revised index, $IC_{revised}$. Both the *IC* and $IC_{revised}$ are used in a qualitative way to compare mean connectivity values at the watershed scale.

In this large territory characterized by diverse landscape types, the *IC* reflects only the high connectivity from hillslope to river network in steep areas while lowland areas appear to be barely connected to the river network. In these areas where hillslope runoff also depends on the soil saturation, a topographic index does not reflect the real sediment connectivity induced by lithological properties. The introduction of the *IDPR* in the $IC_{revised}$ allowed us to consider runoff processes both in steep and flat areas. Changes in connectivity classes induced by this modification affected 51.5 % of the watersheds with 24.1 % of connectivity being increased corresponding to clay-dominated areas, low-permeability areas of the granitic bedrock, and areas with shallow aquifers, and 27.4 % of connectivity being decreased in intensively

fractured bedrock areas and karstified sedimentary formations. Our results also suggest that the *IDPR* cannot be directly used in the model, but first needs to be rescaled to give more weight to the areas characterized by each process. The addition of the *IDPR* values rescaled according to a sigmoid curve has led to a severe decrease in connectivity values in certain regions and to the reclassification of the mean connectivity values (from low to high) of the watersheds. A new map of hillslope connectivity is proposed. The $IC_{revised}$ presents interesting perspectives to define other highly connected areas at the country scale. Indeed, the French territory is a very contrasting landscape which has 29 % of its surface area with slope <2 %, in which 58 % of the area has more runoff properties than infiltration ones (*IDPR* values >1000).

The flexibility of the *IC* seems very promising as it may be able to take into account other distributed parameters such as rainfall intensity or drain tiles. Further research is needed on the connectivity of lowland areas, and the hillslope $IC_{revised}$ proposed in the present study should be coupled to a river index of connectivity and to existing erosion maps (e.g., Cerdan et al. 2010) and compared to suspended sediment fluxes for the same territory (Gay et al. 2014). Finally, the choice was made to aggregate cells into larger units (watersheds). However, other divisions (e.g., Homogeneous Response Units, Bracken et al. 2013) and administrative regions (Le Bissonnais et al. 2002) can be used to provide additional insight into (dis)connected areas according to the decision of stakeholders.

Acknowledgments This work is supported by the Loire Brittany river basin agency (AELB), and the authors would like to thank Xavier Bourrain and Jean-Noël Gautier for funding the VERSEAU project "Transfert de particules des VERSants aux masses d'EAU." The authors would also like to thank Artemi Cerdà and an anonymous reviewer for their interesting comments on the manuscript.

References

Ali GA, Birkel C, Tetzlaff D, Soulsby C, McDonnell JJ, Tarolli P (2013) A comparison of wetness indices for the prediction of observed connected saturated areas under contrasting conditions: wetness indices for the prediction of connected saturated areas. Earth Surf Process Landf 39:399–413

Antoine M, Javaux M, Bielders C (2009) What indicators can capture runoff-relevant connectivity properties of the micro-topography at the plot scale? Adv Water Res 32:1297–1310

Baartman JEM, Masselink R, Keesstra SD, Temme AJAM (2013) Linking landscape morphological complexity and sediment connectivity. Earth Surf Process Landf 38:1457–1471

Bisantino T, Bingner R, Chouaib W, Gentile F, Trisorio Liuzzi G (2015) Estimation of runoff, peak discharge and sediment load at the event scale in a medium-size Mediterranean watershed using the Annagnps model. Land Degrad Dev 26:340–355

Borselli L, Cassi P, Torri D (2008) Prolegomena to sediment and flow connectivity in the landscape: a GIS and field numerical assessment. Catena 75:268–277

Bracken LJ, Croke J (2007) The concept of hydrological connectivity and its contribution to understanding runoff-dominated geomorphic systems. Hydrol Process 21:1749–1763

Bracken LJ, Wainwright J, Ali GA, Tetzlaff D, Smith MW, Reaney SM, Roy AG (2013) Concepts of hydrological connectivity: research approaches, pathways and future agendas. Earth-Sci Rev 119:17–34

Bracken LJ, Turnbull L, Wainwright J, Bogaart B (2015) Sediment connectivity: a framework for understanding sediment transfer at multiple scales. Earth Surf Process Landf 40:177–188

Brierley G, Fryirs K, Jain V (2006) Landscape connectivity: the geographic basis of geomorphic applications. Area 38:165–174

Cavalli M, Trevisani S, Comiti F, Marchi L (2013) Geomorphometric assessment of spatial sediment connectivity in small alpine catchments. Geomorphology 188:31–41

Cerdà A, Doerr SH (2010) The effect of ant mounds on overland flow and soil erodibility following a wildfire in eastern Spain. Ecohydrol 3: 392–401

Cerdan O, Govers G, Le Bissonnais Y, Van Oost K, Poesen J, Saby N, Gobin A, Vacca A, Quinton J, Auerswald K, Klik A, Kwaad FJPM, Raclot D, Ionita I, Rejman J, Rousseva S, Muxart T, Roxo MJ, Dostal T (2010) Rates and spatial variations of soil erosion in Europe: a study based on erosion plot data. Geomorphology 122: 167–177

Chartin C, Evrard O, Onda Y, Patin J, Lefèvre I, Ottlé C, Ayrault S, Lepage H, Bonté P (2013) Tracking the early dispersion of contaminated sediment along rivers draining the Fukushima radioactive pollution plume. Anthropocene 1:23–34

Croke J, Mockler S, Fogarty P, Takken I (2005) Sediment concentration changes in runoff pathways from a forest road network and the resultant spatial pattern of catchment connectivity. Geomorphology 68:257–268

Darboux F, Davy P, Gascuel-Odoux C, Huang C (2001) Evolution of soil surface roughness and flowpath connectivity in overland flow experiments. Catena 46:125–540

Degan F, Cerdan O, Salavador-Blanes S (2015) Cartographie de l'aléa érosif sur le bassin Loire-Bretagne. Technical report. Agence de l'Eau Loire-Bretagne, laboratoire GéoHydrosystèmes COntinentaux de l'Université François Rabelais de Tours, Bureau de Recherches Géologiques et Minières, Orléans, France

Delmas M (2011) Origine des exports de sédiments fluviatiles: prise en compte de l'hétérogénéité spatiale des versants. Unpublished PhD thesis, Université Paris VI, Paris, France

Delmas D, Cerdan O, Mouchel J-M, Garcin M (2009) A method for developing a large scale sediment yield index for european river basins. J Soils Sediments 9:613–626

D'Haen K, Dusar B, Verstraeten G, Degryse P, De Brue H (2013) A sediment fingerprinting approach to understand the geomorphic coupling in an eastern Mediterranean mountainous river catchment. Geomorphology 197:64–75

Dupas R, Delmas M, Dorioz J-M, Garnier J, Moatar F, Gascuel-Odoux C (2015) Assessing the impact of agricultural pressures on N and P loads and eutrophication risk. Ecol Ind 48:396–407

Foerster S, Wilczok C, Brosinsky A, Segl K (2014) Assessment of sediment connectivity from vegetation cover and topography using remotely sensed data in a dryland catchment in the Spanish Pyrenees. J Soils Sediments 14:1982–2000

Foucher A, Salvador-Blanes S, Desmet M, Simonneau A, Chapron E, Evrard O, Courpt T, Cerdan O, Lefèvre I, Adriaensen H, Lecompte F (2015) Increase in after agricultural intensification: evidence from a lowland basin in France. Anthropocene. doi:10.1016/j.ancene.2015.02.001

Fryirs KA, Brierley GJ, Preston NJ, Kasai M (2007) Buffers, barriers and blankets: the (dis)connectivity of catchment-scale sediment cascades. Catena 70:49–67

Gabriels D, Ghekiere G, Schiettecatte W, Rottiers I (2003) Assessment of USLE cover-management C-factors for 40 crop rotation systems on arable farms in the Kemmelbeek watershed, Belgium. Soil Till Res 74:47–53

Gay A, Cerdan O, Delmas M, Desmet M (2014) Variability of suspended sediment yields within the Loire river basin (France). J Hydrol 519: 1225–1237

Gao X, Wu P, Zhao X, Wang J, Shi Y (2014) Effects of land use on soil moisture variation in a semi-arid catchment: implications for land and agricultural water management. Land Degrad Dev 25:163–172

Gumiere SJ, Le Bissonnais Y, Raclot D, Cheviron B (2011) Vegetated filter effects on sedimentological connectivity of agricultural catchments in erosion modelling: a review. Earth Surf Process Landf 36: 3–19

Haregeweyn N, Poesen J, Verstraeten G, Govers G, de Vente J, Nyssen J, Deckers J, Moeyersons J (2013) Assessing the performance of a spatially distributed soil erosion and sediment delivery model (WATEM/SEDEM) in Northern Ethiopia. Land Degrad Dev 24: 188–204

Heckmann T, Schwanghart W (2013) Geomorphic coupling and sediment connectivity in an alpine catchment – Exploring sediment cascades using graph theory. Geomorphology 182:89–103

Horton RE (1945) Erosional development of streams and their drainage basins; hydrophysical approach to quantitative morphology. Geol Soc Am Bull 56:275

Kiesel J, Schmalz B, Fohrer N (2009) SEPAL-a simple GIS-based tool to estimate sediment pathways in lowland catchments. Adv Geosci 21: 25–32

Kiesel J, Fohrer N, Schmalz B, White MJ (2010) Incorporating landscape depressions and tile drainages of a northern german lowland catchment into a semi-distributed model. Hydrol Process 24:1472–1486

Kirkby M (2014) Do not only connect: a model of infiltration-excess overland flow based on simulation. Earth Surf Process Landf 39: 952–963

Landemaine V, Gay A, Cerdan O, Salvador-Blanes S, Rodrigues S (2015) Morphological evolution of a rural headwater stream after channelisation. Geomorphology 230:125–137

Lane SN, Reaney SM, Heathwaite AL (2009) Representation of landscape hydrological connectivity using a topographically driven surface flow index. Water Resour Res 45, W08423. doi:10.1029/2008WR007336

Le Bissonnais Y, Montier C, Jamagne M, Daroussin J, King D (2002) Mapping erosion risk for cultivated soil in France. Catena 46:207–220

Le Bissonnais Y, Cerdan O, Lecomte V, Benkhadra H, Souchère V, Martin P (2005a) Variability of soil surface characteristics influencing runoff and interrill erosion. Catena 62(2–3):111–124

Le Bissonnais Y, Jamagne M, Lambert JJ, Le Bas C, Daroussin J, King D, Cerdan C, Léonard J, Bresson LM, Jones R (2005b) Pan-European soil crusting and erodibility assessment from the European soil geographical database using pedotransfer rules. Adv Environ Monit Model 2:1–15

López-Vicente M, Navas A, Gaspar L, Machín J (2013) Advanced modelling of runoff and soil redistribution for agricultural systems: the SERT model. Agric Water Manag 125:1–12

Mardhel V, Frantar P, Uhan J, Andjelov M (2004) Index of development and persistence of the river networks (IDPR) as a component of regional groundwater vulnerability assessment in Slovenia. In Proceedings on the International Conference on Groundwater vulnerability assessment and mapping, Ustron, Poland, pp 15–18

Mardhel V, Gravier A (2006) Carte de vulnérabilité simplifiée des eaux souterraines du bassin Loire Bretagne. Technical Report BRGM/RP-54553-FR, BRGM, Paris

Mekonnen M, Keesstra SD, Stroosnijder L, Baartman JEM, Maroulis J (2014) Soil conservation through sediment trapping: a review. Land Degrad Dev. doi:10.1002/ldr.2308

Meßenzehl K, Hoffmann T, Dikau R (2014) Sediment connectivity in the high-alpine valley of Val Müschauns, Swiss National Park - linking geomorphic field mapping with geomorphometric modelling. Geomorphology 221:215–229

Novara A, Gristina L, Saladino SS, Santoro A, Cerdà A (2011) Soil erosion assessment on tillage and alternative soil managements in a Sicilian vineyard. Soil Till Res 117:140–147

Reid SC, Lane SN, Montgomery DR, Brookes CJ (2007) Does hydrological connectivity improve modelling of coarse sediment delivery in upland environments? Geomorphology 90:263–282

Renard KG, Foster GR, Weesies GA, McCool DK, Yoder DC (1997) Predicting soil erosion by water: a guide to conservation planning with the revised universal soil loss equation (RUSLE). Agriculture Handbook 703. US Department of Agriculture, Washington

Russell MA, Walling DE, Hodgkinson RA (2001) Suspended sediment sources in two small lowland agricultural catchments in the UK. J Hydrol 252:1–24

Sougnez N, van Wesemael B, Vanacker V (2011) Low erosion rates measured for steep, sparsely vegetated catchments in southeast Spain. Catena 84:1–11

Van Oost K, Govers G, Desmet P (2000) Evaluating the effects of changes in landscape structure on soil erosion by water and tillage. Landsc Ecol 15:577–589

Vigiak O, Borselli L, Newham LTH, McInnes J, Roberts AM (2012) Comparison of conceptual landscape metrics to define hillslope-scale sediment delivery ratio. Geomorphology 138: 74–88

Vogt J, Soille P, de Jager A, Rimaviciuté E, Mehl W, Foisneau S, Bodis K, Dusart J, Paracchini ML, Haastrup P, Bamps C (2007) A pan-European river and catchment database. European Commission, EUR 22920 EN – Joint Research Centre – Institute for Environment and Sustainability. Office for Official Publications of the European Communities, Luxembourg, p 120

Walling DE (1983) The sediment delivery problem. J Hydrol 65:209–237

Walling DE, Collins AL (2008) The catchment sediment budget as a management tool. Environ Sci Policy 11:136–143

Western AW, Blöschl G, Grayson RB (2001) Toward capturing hydrologically significant connectivity in spatial patterns. Water Resour Res 37:83–97

Wischmeier WH, Smith DD (1978) Predicting rainfall erosion losses-a guide to conservation planning. Agricultural Handbook 537. US Department of Agriculture, Washington